Atmospheric Environment 77 (2013) 453–463

Contents lists available at SciVerse ScienceDirect

Atmospheric Environment

journal homepage: www.elsevier.com/locate/atmosenv

Impact of national NO_x and SO_2 control policies on particulate matter pollution in China

Bin Zhao [a], Shuxiao Wang [a,b,*], Jiandong Wang [a], Joshua S. Fu [c], Tonghao Liu [a], Jiayu Xu [a,b], Xiao Fu [a], Jiming Hao [a,b]

[a] School of Environment, State Key Joint Laboratory of Environment Simulation and Pollution Control, Tsinghua University, Beijing 100084, China
[b] State Environmental Protection Key Laboratory of Sources and Control of Air Pollution Complex, Beijing 100084, China
[c] Department of Civil and Environmental Engineering, University of Tennessee, TN 37996, USA

HIGHLIGHTS

- The effects of China's NO_x and SO_2 control policies on PM pollution are assessed.
- NO_x and SO_2 emissions in 2015 decrease by 23.4% and 18.9% from baseline projection.
- Annual $PM_{2.5}$ concentration declines 1.5–6 μg m^{-3} under national NO_x control policy.
- Annual $PM_{2.5}$ concentration declines 3–8.3 μg m^{-3} under joint NO_x and SO_2 controls.
- Current policies are not enough to improve the air quality in key regions of China.

ARTICLE INFO

Article history:
Received 5 December 2012
Received in revised form
10 April 2013
Accepted 6 May 2013

Keywords:
Particulate matter
12th Five Year Plan
NO_x emissions
SO_2 emissions
WRF/CMAQ
Scenario analysis

ABSTRACT

China's air pollution control policies during the 12th Five Year Plan (2011–2015) are characterized by the targets of 10% nitrogen oxides (NO_x) reduction and 8% sulfur dioxide (SO_2) reduction from the 2010 levels. In this study, the Community Multi-scale Air Quality (CMAQ) modeling system was used to evaluate the impact of only SO_2, only NO_x, and joint SO_2/NO_x control measures on particulate matter pollution, the greatest concern for urban air quality in China. Four emission scenarios were developed for 2015, including a business-as-usual scenario, a reference NO_x control scenario based on the governmental plan, an accelerated NO_x control technology scenario, and a scenario assuming joint controls of NO_x and SO_2 based on the governmental plan. Under the planned NO_x control measures, the annual mean concentrations of particulate matter less than or equal to 2.5 μm ($PM_{2.5}$) decline by 1.5–6 μg m^{-3}, i.e. 1.6%–8.5%, in the majority of eastern China. The largest reduction occurs in the middle reach of the Yangtze River. Under accelerated NO_x control measures, the annual average $PM_{2.5}$ concentration reductions (compared with the business-as-usual scenario) in eastern China are 65% higher than the reductions under planned control measures. The unusual increase of $PM_{2.5}$ concentrations in the North China Plain and the Yangtze River Delta during January after the reductions of NO_x emissions was an integrated effect of excessive NO_x, the ammonia-rich inorganic aerosol chemistry, and the non-methane volatile organic compounds (NMVOC) sensitive photochemical regime. Under the joint controls of NO_x and SO_2, the annual mean $PM_{2.5}$ concentrations decline over 3 μg m^{-3}, i.e. 3.2%–13%, in the majority of eastern China, and some areas in the middle reach of the Yangtze River have reductions as large as 6–8.3 μg m^{-3}, i.e. 5.0%–13%. The average $PM_{2.5}$ concentration reductions in eastern China are 1.20 μg m^{-3}, 3.14 μg m^{-3}, 3.57 μg m^{-3}, 4.22 μg m^{-3} in January, May, August, and November, respectively. The corresponding declining rates are 2.3%, 12.2%, 14.3%, and 8.1%, respectively. More stringent policies should be implemented in winter to reduce the heavy pollution periods. The annual average $PM_{2.5}$ concentration reductions in three major city clusters are comparable with the average reductions of eastern China. Stringent regional control policies are required for the significant improvement of particulate air quality in major city clusters.

* Corresponding author. School of Environment, State Key Joint Laboratory of Environment Simulation and Pollution Control, Tsinghua University, Beijing 100084, China.
E-mail address: shxwang@tsinghua.edu.cn (S. Wang).

1352-2310/$ – see front matter © 2013 Published by Elsevier Ltd.
http://dx.doi.org/10.1016/j.atmosenv.2013.05.012

1. Introduction

Driven by rapid economic development and intensive energy use, emissions of atmospheric pollutants have caused severe particulate matter pollution in China. With inversion method based on satellite data, the concentrations of particulate matter less than or equal to 2.5 μm ($PM_{2.5}$) were estimated to be over 80 μg m^{-3} in Eastern China (van Donkelaar et al., 2010). Particulate matter, especially $PM_{2.5}$, not only worsens the visibility (Zhang et al., 2012), but also significantly affects climate (Solomon et al., 2007) and public health (WB and SEPA, 2007).

During the 11th Five Year Plan (2006–2010), the Chinese government had taken aggressive steps to improve energy efficiency and reduce emissions of primary aerosols and SO_2. Small, inefficient power generating units and industrial facilities were replaced with larger and more efficient ones. The ratio of thermal power plants equipped with flue gas desulfurization (FGD) increased from 12% in 2005 to 82.6% in 2010 (http://www.gov.cn/zwgk/2011-12/20/content_2024895.htm). Consequently, the emissions of total suspended particulate (TSP) and SO_2 decreased from 2005 to 2010 by 39.0% and 14.3%, respectively (Chinese Environmental Statistical Bulletin, http://www.mep.gov.cn/zwgk/hjtj/). Attributable to the emission reductions, the annual average concentrations of particulate matter less than or equal to 10 μm (PM_{10}) in 86 key cities decreased from 96.7 μg m^{-3} in 2005 to 88.1 μg m^{-3} in 2010 (http://datacenter.mep.gov.cn). However, satellite-based Aerosol Optical Depth (AOD) observations indicated the control policies had not been successful in reducing concentrations of $PM_{2.5}$ or finer particles over industrialized regions of China. The lack of success can be partly explained by the increasing importance of anthropogenic secondary aerosols formed from precursor species including SO_2, NO_x, NMVOC, and NH_3 (Lin et al., 2010).

In an attempt to improve the air quality further, the Chinese government published the "Twelfth Five Year Plan for National Environment Protection" in 2011 (http://www.gov.cn/zwgk/2011-12/20/content_2024895.htm). The plan aimed to reduce NO_x and SO_2 emissions by 10% and 8% by 2015 from the 2010 levels. Along with the objectives, the plan included a detailed roadmap to achieve the objective, targeting emissions from the power plants, steel and cement industry, industrial boilers, transportation, etc.

The purpose of this study is to assess the impact of SO_2, NO_x, and joint SO_2/NO_x emission control measures on particulate matter pollution in China during the 12th Five Year plan. Emission inventory lays the basis for such an assessment. The most recently published emission inventories of China include a 2005 inventory developed by Wang et al. (2011a), and a 2006 inventory by Zhang et al. (2009), both of which are in good accuracy but cannot reflect the dramatic changes during 2006–2010. There have been a number of numerical studies on air pollution control policies in the literature, most of these studies focus on the evaluation of pollution control efforts at city or regional scale, e.g. the Beijing city (Streets et al., 2007; Wang et al., 2010c), the Yangtze River Delta (Li et al., 2011), the Pearl River Delta (Wei et al., 2007), and Shangdong (Wang et al., 2005) and Hebei (Wang et al., 2012) provinces. Wang et al. (2010a,b) calculated the changes of annual average SO_2, NO_x, and $PM_{2.5}$ concentrations at the national level because of SO_2 or NO_x emission control measures during 2005–2010. This manuscript, compared with previous studies, developed a new multiple pollutant emission inventory for year 2010 and evaluated the impacts of only SO_2, only NO_x, and joint SO_2/NO_x control scenarios on different particulate matter species over both national and regional scales in different seasons. We focus on how the different chemistry mechanisms in various seasons and regions affect the effectiveness of control measures, which had important policy implications but have not been reported in previous studies.

2. Emission inventory and scenarios

2.1. Emission inventory for 2010

We present an emission inventory of SO_2, NO_x, PM_{10}, $PM_{2.5}$, black carbon (BC), organic carbon (OC), NMVOC, and NH_3 for China for the year 2010 for the first time. To develop this inventory, an "emission factor method" was used to calculate air pollutant emissions, as described in detail in Wang et al. (2011a). The emissions (except BC/OC) from each sector in each province were calculated from the activity data (energy consumption, industrial products, solvent use, etc.), technology-based uncontrolled emission factors, and penetrations of control technologies. The emissions of BC and OC were estimated based on $PM_{2.5}$ emissions and the ratio of BC/OC to $PM_{2.5}$ emissions. The activity data, and technology distribution for each sector were derived based on the Chinese Statistics (NBS, 2011a,b,c; China Association of Automobile Manufacturers, 2011), a wide variety of Chinese technology reports (China Electricity Council, 2011; ERI, 2009, 2010; THUBERC, 2009; Wang, 2011), and an energy demand modeling approach. The emission factors used by Wang et al. (2011a) were reanalyzed to incorporate the latest field measurements. The uncontrolled emission factors adopted in this inventory, as well as the ratio of BC/OC to $PM_{2.5}$, are summarized in Tables S1–S4. The penetrations of removal technologies (summarized in Tables S7–S10) were updated to 2010 according to the governmental bulletin (MEP, 2011), the evolution of emission standards, and a variety of technical reports. A unit based method was applied to estimate the emissions from large point sources including coal-fired power plants, iron and steel plants, and cement plants (Lei et al., 2011; Wang et al., 2011a; Zhao et al., 2008).

In 2010, the anthropogenic emissions of SO_2, NO_x, PM_{10}, $PM_{2.5}$, BC, OC, NMVOC and NH_3 in China were estimated to be 24.4 Mt, 26.1 Mt, 15.8 Mt, 11.8 Mt, 1.93 Mt, 3.51 Mt, 22.9 Mt, and 18.3 Mt, respectively. Compared with the emissions of 2005, the corresponding change rates were −14.9%, 33.8%, −15.1%, −11.7%, −0.9%, −5.3%, 21.0%, and 10.4%, respectively. The emissions by sector are given in Table S5, and emissions by province are given in Table 1. The method and parameters for spatio-temporal distributions of anthropogenic emissions, speciation of NMVOC emissions, and calculation of biogenic NMVOC emissions are described in our previous paper (Wang et al., 2011a).

2.2. Emission scenarios for 2015

The energy consumption and NO_x/SO_2 emissions in 2015 were projected with a detailed, consistent, and dynamic technology-based model framework (Zhao et al., 2013). The driving forces (e.g. GDP, population) are forecasted first, then energy service demand is forecasted based on driving forces. The future technology distribution and energy efficiencies are assumed and the energy consumption is calculated. Finally, air pollutant emissions are derived from energy consumption, emission factors and assumptions on the penetration of control technologies. All of the emission scenarios developed in this study incorporated the same energy scenario, which was developed based on the governmental plan concerning economic development and energy conservation. The Chinese government released the "Twelfth Five Year Plan for National Economic and Social Development" (http://news.xinhuanet.com/politics/2011-03/16/c_121193916.htm) in 2011, in which the annual average GDP growth rate is expected to be 7% (we adopted 8% in our scenario since the actual GDP growth rate was 2.5%–3.7% higher than the governmental target in the last two Five Year Plans). The energy consumption and CO_2 emissions per GDP are expected to decrease from 2010 to 2015 by 16% and 17%, respectively. The major assumptions of the energy scenario

Table 1
Summary of the air pollutants emissions by province in 2010 (units, kt year^{-1}).

	SO_2	NO_x	PM_{10}	$PM_{2.5}$	BC	OC	NMVOC	NH_3
Beijing	325.2	475.3	127.6	88.6	18.0	15.4	371.0	84.0
Tianjin	331.5	408.2	151.0	114.5	18.0	27.4	294.8	96.8
Hebei	1163.8	1622.4	1146.4	860.6	143.5	220.0	1438.7	1063.2
Shanxi	1023.2	1052.7	628.7	470.6	105.1	129.3	640.3	287.4
Inner Mongolia	1053.6	1160.5	553.9	412.8	89.8	120.3	569.3	593.2
Liaoning	953.7	1145.1	610.1	461.6	71.6	134.8	904.7	589.1
Jilin	401.0	638.9	452.3	341.1	54.5	104.2	458.8	528.0
Heilongjiang	283.2	717.7	497.3	396.8	63.8	157.3	576.4	493.1
Shanghai	620.3	468.0	160.0	112.0	12.5	10.5	541.4	61.8
Jiangsu	1185.1	1747.6	968.7	702.7	88.2	175.6	1933.1	1132.8
Zhejiang	1592.0	1266.7	485.3	327.1	37.4	53.1	1586.1	365.2
Anhui	575.9	990.3	783.6	609.4	97.9	234.0	1040.9	1009.4
Fujian	554.8	729.9	302.3	216.1	29.1	52.3	633.0	367.9
Jiangxi	389.6	499.2	383.9	261.3	36.7	69.9	458.8	477.0
Shandong	2464.9	2515.3	1396.9	1025.7	168.1	263.9	2254.4	1586.5
Henan	1187.2	1859.9	1148.7	846.6	123.1	226.4	1359.6	2007.0
Hubei	1182.1	961.5	774.7	568.7	108.3	175.7	910.5	980.8
Hunan	849.4	840.0	700.8	510.0	84.4	148.3	756.5	853.8
Guangdong	1258.6	1762.5	713.3	507.3	66.8	136.3	1600.5	893.0
Guangxi	798.0	582.4	587.8	456.2	52.4	153.7	736.4	806.6
Hainan	75.1	92.9	55.4	42.9	5.0	14.8	133.0	160.5
Chongqing	1201.3	461.3	316.0	233.4	39.3	74.5	402.7	367.2
Sichuan	1708.8	978.2	852.1	667.9	104.4	272.2	1279.0	1188.8
Guizhou	953.5	517.3	445.8	353.0	81.5	138.4	349.8	388.4
Yunnan	434.3	515.8	433.1	329.3	68.9	114.1	434.2	654.7
Tibet	4.9	24.6	10.0	8.2	1.3	2.8	15.8	43.8
Shaanxi	726.8	682.1	401.8	311.3	58.4	115.0	471.7	402.1
Gansu	276.0	455.8	245.1	193.0	34.4	66.8	247.1	250.9
Qinghai	42.1	89.9	62.6	48.1	9.4	12.8	53.1	80.2
Ningxia	266.6	301.7	119.4	84.3	12.4	14.9	81.5	97.8
Xinjiang	540.2	491.3	292.9	225.3	41.9	72.3	326.6	401.4
Total	24422.7	26054.9	15807.3	11786.2	1925.9	3506.9	22859.7	18312.3

are summarized in Table S6. In 2015, the total energy consumption in China is projected to increase to 4999 Mtce, 20.2% larger than that of 2010. The energy consumption by fuel and by sector is given in Fig. S1.

We developed four emission scenarios for the energy scenario, including a business-as-usual scenario (BAU scenario), a reference NO_x control scenario (REF scenario), an accelerated NO_x control technology scenario (ACT scenario), and a scenario for the joint controls of NO_x and SO_2 (REF_SC scenario). The BAU scenario assumes that all current legislation (until the end of 2010) and the current implementation status would be followed during 2011–2015. The REF scenario assumes the NO_x control policies in the "Twelfth Five Year Plan for National Environment Protection" (the "Plan") would be implemented, representing our "best guess" of future NO_x emissions. The "Plan" requests all new-built power generation units and large existing units ($\geq$300 MW) to be equipped with flue gas denitrification equipment. Control measures on industrial boilers, cement and steel industry, and transportation are also requested. The ACT scenario assumes that more stringent NO_x control policies would be released and implemented. As for power plants, a new emission standard issued in 2011 is expected to be carried out stringently. The new standard requests nearly all thermal power plants to be equipped with Selective Catalytic Reduction (SCR) system. While the three scenarios above assume current legislation (until the end of 2010) for SO_2 control, the REF_SC scenario assumes both the NO_x and SO_2 control policies in the "Plan" to be implemented, representing our "best guess" of both NO_x and SO_2 emissions. The SO_2 control policies during the 11th Five Year Plan focused on power plants. In contrast, the policies of the 12th Five Year Plan extend to a variety of sectors, including power plants, iron and steel industry, industrial boilers, etc. The penetrations of major removal technologies of each emission scenario are summarized in Tables S7, S8 and S10.

Fig. 1 summarizes the national anthropogenic emissions of SO_2 and NO_x for each scenario, and Table S11 shows the provincial emissions. In 2015, the total NO_x emissions are projected to be 29.8 Mt, 22.9 Mt, and 19.8 Mt under BAU, REF, and ACT scenarios, respectively. The corresponding change rates compared with 2010 are 14.5%, −12.2%, and −23.9%, respectively. Although the REF scenario was designed based on the governmental plan, the NO_x emission reduction rate of 12.2% exceeded the target of 10%, because the government set up a strict and detailed control plan to guarantee the fulfillment of the target. The SO_2 emissions are expected to increase by 11.4% in 2015 from the 2010 levels under current legislations. If the national SO_2 control policy is implemented successfully, the total SO_2 emissions in 2015 are projected to decline by 9.6% from the 2010 levels, and 18.9% from the 2015_BAU scenario. Fig. 1 also illustrates the relative contributions of each sector to total SO_2 and NO_x emissions. For example, the share of power plants in total NO_x emissions decreases from 31% in 2010 to 14% in the 2015_ACT scenario.

3. Model configuration and evaluation

3.1. Model configuration

The Community Multi-scale Air Quality (CMAQ) modeling system version 4.7.1 was used to evaluate the impact of NO_x and SO_2 emission controls on air quality in China. The modeling domain covered most of China and part of East Asia with a 36 km $\times$ 36 km grid resolution, as shown in Fig. 2. The region-specific analysis included four typical regions: the Eastern China (ECH), the North China Plain (NCP), the Yangtze River Delta (YRD), and the Pearl River Delta (PRD). A Lambert projection with the two true latitudes of 25 N and 40 N was used. The domain origin was (34_N, 110_E), and the coordinates of the southwest corner were ($x = -2934$ km,

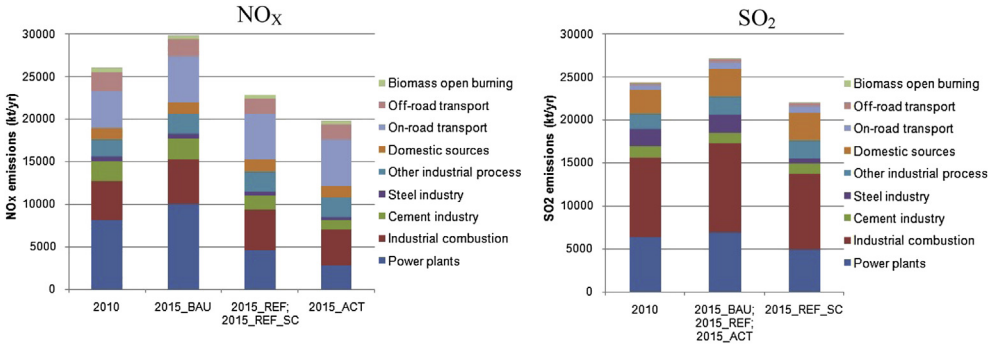

Fig. 1. SO_2 and NO_x emissions by sector in China in 2010 and 2015.

$y = -1728$ km). The selected model simulation periods include January, May, August and November, 2010 and 2015, representing the four seasons in 2010 and 2015.

The Weather Research and Forecasting Model (WRF, version 3.3) was used to generate the meteorological fields. The Meteorology–Chemistry Interface Processor (MCIP) version 3.6 was applied to process the meteorological data in a format required by CMAQ. The same meteorological field generated by WRF for the base year 2010 was used for all the 2015 scenarios. CMAQ was configured using the AERO5 aerosol module and the CB-05 gas-phase chemical mechanism. A description of the configurations of WRF, the treatment of aerosol physics and chemistry, and the treatment of dry and wet depositions is provided in the Supplementary Information. The configurations of vertical resolution, initial conditions, and boundary conditions are consistent with our previous paper (Wang et al., 2010c).

3.2. Evaluation of the modeling system

The meteorological predictions were evaluated against observational data from the National Climatic Data Center (NCDC), and the air quality predictions were evaluated against both surface observations and satellite observations. The evaluation of meteorology and air quality predictions is described in detail in the Supporting Information. The simulated wind speed, wind direction, temperature, and humidity show good agreement with the NCDC observations (Table S12). The simulated NO_2 vertical column density and AOD can generally capture the spatial and seasonal trends observed by Ozone Monitoring Instrument (OMI) and Moderate Resolution Imaging Spectroradiometer (MODIS) (Figs. S2, S3, and Table S13). The comparison of simulated PM_{10} concentrations with the observations of over 86 major cities shows an underestimation of 14%–42% in ECH, attributable to the exclusion of fugitive dust emissions, and the underestimation of secondary organic aerosols (SOA). The statistical indices are generally within the benchmark values. The modeling system can capture the temporal variation of $PM_{2.5}$ concentrations fairly well in Miyun site (40.48°N, 116.78°E, at an altitude of 152 m, see Fig. 2) and Chongming site (31.52°N, 121.91°E, at an altitude of 2 m, see Fig. 2). The simulated monthly average concentrations are comparable with observations in Miyun site, with NMBs ranging from −15% to 1%. The simulation at Chongming site also agrees well with the observations, although it tends to underestimate the $PM_{2.5}$ concentration in May, with a NMB of −32% (see Fig. 3).

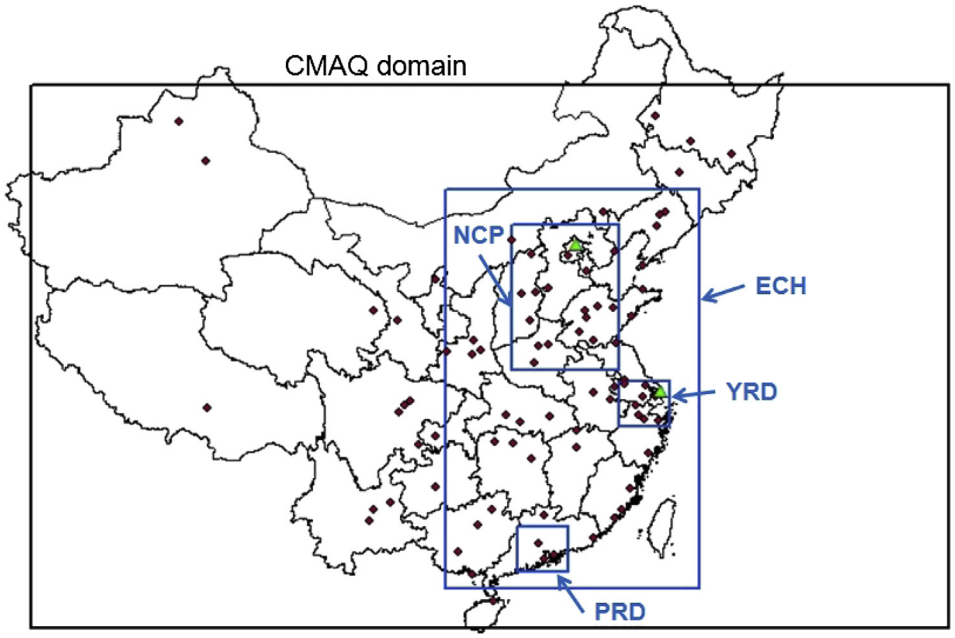

Fig. 2. The CMAQ modeling domain at a horizontal grid resolution of 36 km (164 × 97 cells), and the locations of the four typical regions, i.e. ECH, NCP, YRD, and PRD. The two green triangles indicate the locations of Miyun (north) and Chongming (south) site. The purple points indicate the 86 major cities monitored by the Ministry of Environmental Protection of China. (For interpretation of the references to color in this figure legend, the reader is referred to the web version of this article.)

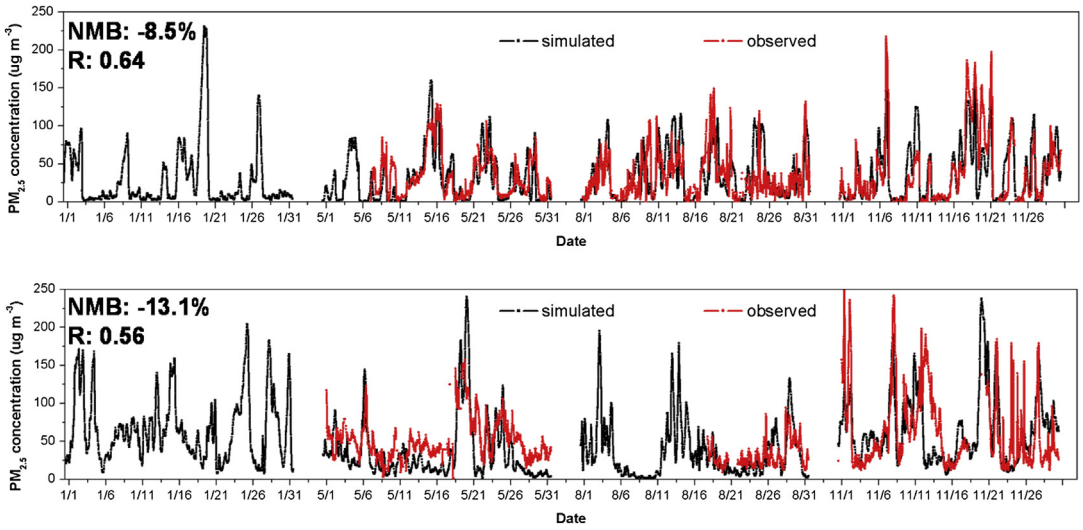

Fig. 3. Comparison of the simulated $PM_{2.5}$ concentrations with the observations in Miyun site (top) and Chongming site (bottom).

4. Impact of NO_x and SO_2 controls on particulate matter pollution

4.1. Impact of NO_x controls on particulate matter pollution

Compared with the 2015_BAU scenario, the NO_x emissions are expected to be reduced by 23.4% and 33.6% under the 2015_REF and 2015_ACT scenarios, respectively. Fig. 4 illustrates the $PM_{2.5}$ concentrations under the 2015_BAU scenario and 2015_REF scenario, and the reduction of $PM_{2.5}$ concentration from the 2015_BAU scenario to the 2015_REF scenario. It can be seen that the $PM_{2.5}$ concentrations of eastern China are significantly higher than those of other regions; the most polluted regions include NCP, YRD, the middle reach of the Yangtze River (mainly Hubei and northern Hunan provinces), the Sichuan Basin, and PRD. This spatial distribution has a similar pattern to that of the primary pollutant emissions (Figs. S4 and S6). Due to the planned NO_x controls, the annual mean $PM_{2.5}$ concentrations decline by 1.5–6 μg m^{-3}, i.e. 1.6%–8.5%, in the majority of ECH. The largest reduction (4.5–6 μg m^{-3}, i.e. 4.7%–8.5%) occurs in the middle reach of the Yangtze River. The annual average $PM_{2.5}$ concentration reductions are 1.81 μg m^{-3}, 1.91 μg m^{-3}, 1.72 μg m^{-3}, and 1.44 μg m^{-3} in ECH, NCP, YRD, and PRD, respectively, as shown in Table 2. The corresponding declining rates are 4.6%, 3.4%, 2.6%, and 4.0%, respectively. The reductions in the three city clusters are comparable with the reductions in other parts of the eastern China, implying that the nation-wide NO_x emission reductions are not enough for significant improvement of the urban air quality in the key regions.

The average $PM_{2.5}$ concentration reductions in ECH were 0.50 μg m^{-3}, 1.81 μg m^{-3}, 1.96 μg m^{-3}, and 2.97 μg m^{-3} in January, May, August, and November, respectively. The corresponding declining rates are 0.9%, 7.0%, 7.8%, and 5.7%, respectively. This seasonal variation is an integrated effect of different meteorological conditions and chemical mechanisms in different seasons. As a result of NO_x emission reductions, the concentrations of nitrate and ammonium decrease, while the sulfate concentrations increase inversely due to thermodynamic effects. The reductions of nitrate concentrations dominate the reductions of $PM_{2.5}$ concentrations (see Table 3). In January and November, the average nitrate concentration in ECH is evidently higher than that of the other two months (Fig. S5), as high temperature favors the evaporation of nitrate. This supports the finding that the largest $PM_{2.5}$ concentration reduction occurs in November. The reasons for the smaller reduction in January are described in detail in the following paragraphs. Consistent with the spatial pattern of nitrate concentrations, the largest $PM_{2.5}$ concentration reduction (in January and November) occurs in the middle reach of the Yangtze River and the Sichuan Basin, attributable to favorable temperatures and the transport of particulate matter and its precursors from northern China (driven by northerly monsoon). Also note that the $PM_{2.5}$ concentrations increase in NCP and YRD during January, and in NCP during November. The underlying reasons will be explained in the following paragraphs. In comparison, the $PM_{2.5}$ concentration reductions are moderate in May and August. The largest reduction occurs in NCP, attributable to the southerly monsoon and excessively high temperature in southern China.

It is mentioned above that the $PM_{2.5}$ concentrations increase in NCP and YRD during January due to the reductions of NO_x emissions. Below we analyze the chemical mechanism underlying this special phenomenon. The inorganic aerosol chemistry differs greatly under the NH_3-rich and NH_3-poor conditions. Indicators such as the degree of sulfate neutralization (DSN) and gas ratio (GR) could be used to identify the NH_3-poor, -neutral, or -rich condition, then to determine the sensitivity of inorganic aerosols to precursors' emissions (Wang et al., 2011b). Their definitions are given as follows:

$$\mathrm{DSN} = \frac{\left[\mathrm{NH_4^+}\right] - \left[\mathrm{NO_3^-}\right]}{\left[\mathrm{SO_4^{2-}}\right]} \quad (1)$$

$$\mathrm{GR} = \frac{\left([\mathrm{NH_3}] + \left[\mathrm{NH_4^+}\right]\right) - 2 \times \left[\mathrm{SO_4^{2-}}\right]}{\left[\mathrm{NO_3^-}\right] + [\mathrm{HNO_3}]} \quad (2)$$

The simulated DSN is approximately equal to 2, and GR is evidently larger than 1 (see Table 4), implying that both NCP and YRD are under NH_3-rich condition in January. This conclusion is consistent with Wang et al. (2011b). Therefore, the formation of inorganic aerosols is sensitive to abundance of SO_2, NO_x, and oxidants (O_3, HO_x radical). Following the NO_x emission reductions, sulfate concentrations increase in both NCP and YRD, due primarily to the increase of O_3 and HO_x radical (see Table 4). The nitrate concentration decreases over YRD, which is nevertheless compensated by the increase of sulfate and ammonium, leading to

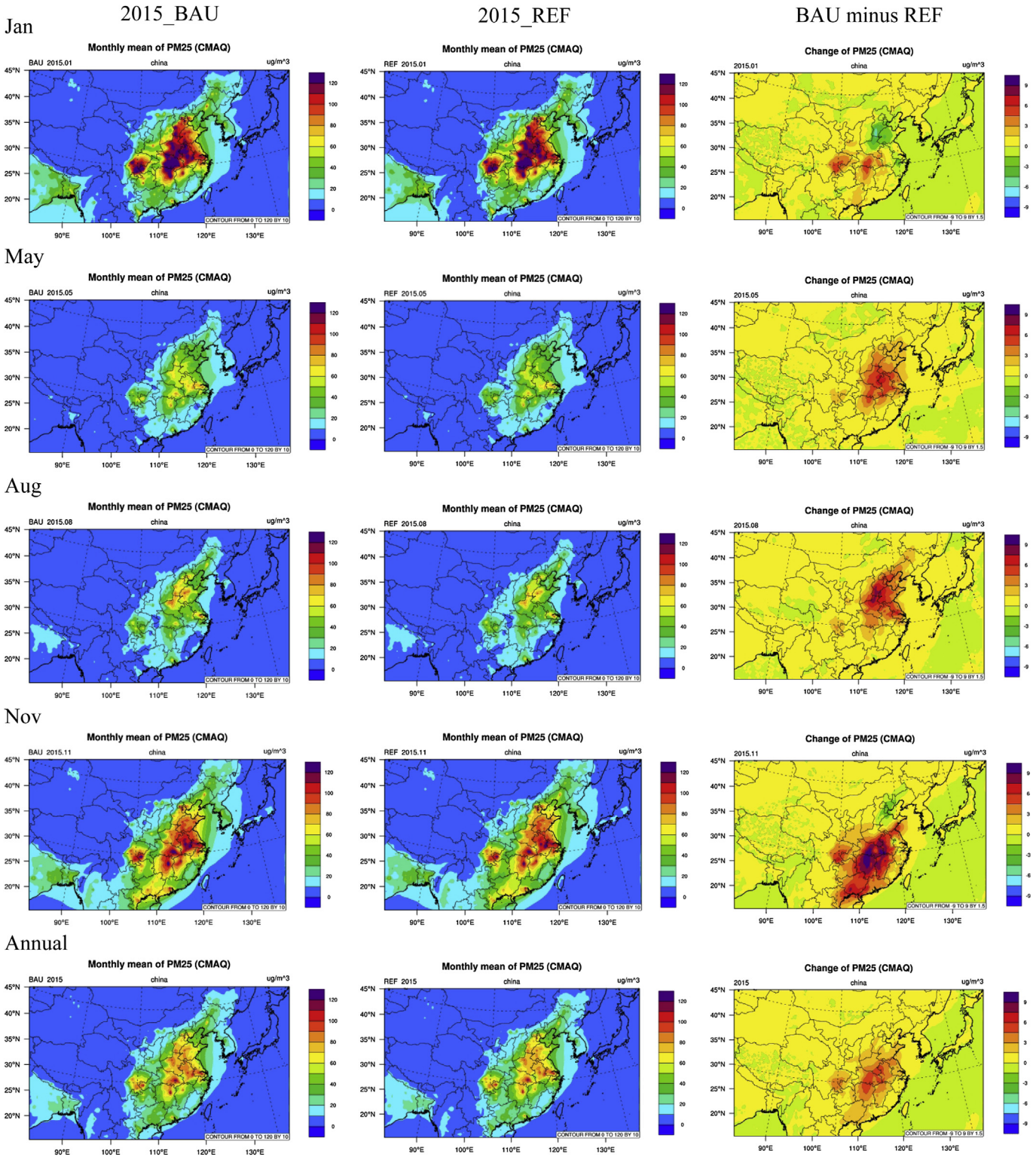

Fig. 4. Spatial distribution of the monthly (Jan, May, Aug, Nov) and annual mean $PM_{2.5}$ concentrations under the 2015_BAU scenario (left column), the 2015_REF scenario (middle column), and the reductions of $PM_{2.5}$ concentrations from the 2015_BAU scenario to the 2015_REF scenario (BAU minus REF, right column).

Table 2
The annual mean concentrations of $PM_{2.5}$ in 2010 and under four scenarios in 2015 (BAU, REF, ACT, REF_SC) over ECH, NCP, YRD, and PRD, and the reductions between different scenarios (unit: μg m^{-3}).

	ECH	NCP	YRD	PRD
2010	37.70	55.19	65.77	34.10
2015_BAU	39.06	56.64	67.14	35.58
2015_REF	37.25	54.72	65.42	34.14
2015_ACT	36.07	53.37	64.00	33.47
2015_REF_SC	36.03	53.12	63.15	32.78
BAU minus REF	1.81 (−0.04–5.90)	1.91 (0.30–5.13)	1.72 (0.69–3.11)	1.44 (0.82–3.20)
BAU minus ACT	2.99 (−0.05–9.83)	3.27 (0.51–8.57)	3.15 (1.45–5.41)	2.11 (1.20–4.49)
BAU minus REF_SC	3.03 (0.07–8.23)	3.52 (0.56–7.28)	3.99 (1.96–7.22)	2.80 (1.72–4.94)
REF minus REF_SC	1.23 (0.07–5.16)	1.60 (0.26–3.76)	2.27 (1.01–5.16)	1.36 (0.90–2.25)

an overall increase of $PM_{2.5}$ concentrations. In contrast, the nitrate concentrations increase in NCP with the reductions of NO_x emissions. The formation of nitrate is more sensitive to HNO_3 due to the NH_3-rich chemistry. The formation pathway of HNO_3 is dominated by reaction (3) in the daytime, and reactions (4)–(6) at night (Seinfeld and Pandis, 2006):

$$NO_2 + OH + M \rightarrow HNO_3 + M \quad (3)$$

$$NO_2 + O_3 \rightarrow NO_3 + O_2 \quad (4)$$

$$NO_2 + NO_3 + M \rightarrow N_2O_5 + M \quad (5)$$

$$N_2O_5 + H_2O(s) \rightarrow 2HNO_3 \quad (6)$$

Both pathways are influenced by the abundance of oxidants, products of photochemistry. We introduced a photochemical indicator proposed by Sillman (1995), $H_2O_2/(HNO_3+NO_3^-)$. Its simulated values (0.02–0.04, shown in Table 4) are different enough from the thresholds of 0.9 (Lu and Chang, 1998) to determine that O_3 concentrations should be sensitive to NMVOC emissions in both NCP and YRD in January. A more important implication is that HO_x radical is an important limiting factor for the product of HNO_3, as the HO_2 radical termination product (H_2O_2) accounts for only 2%–4% of the OH + NO_2 termination product ($HNO_3+NO_3^-$). The NO_x emission reductions result in an elevated level of O_3 and HO_x radical (see Table 4), then enhancing both the HNO_3 formation through OH + NO_2 collision in the daytime, and the NO_3 and N_2O_5 formation through oxidation of NO_2 by O_3 at night. The enhancing oxidants compensated the decrease of NO_x concentration, leading to more formation of HNO_3 and NO_3^- (illustrated by the increase of TN = $HNO_3+NO_3^-$ in Table 4).

Similar mechanisms underlie the smaller $PM_{2.5}$ concentration reductions in ECH during January compared with November. The NO_x emission reductions lead to the enhancement of atmospheric oxidation capacities both in January and November, indicated by the increase of O_3 and HO_x radical (see Tables 3 and 4). But this "titration effect" is more significant in January than in November, as concluded from the results that average O_3 concentrations in ECH increase by 9.0% and 5.8%, and HO_x concentrations increased by 27% and 14% in January and November, respectively. Lower temperature lowers the photochemical reactions in January, resulting in less HO_x radical and more free NO_x consuming HO_x, and consequently larger "titration effect". The enhanced oxidation capacity favors the formation of sulfate and nitrate. Moreover, lower temperature favors the heterogeneous reaction of N_2O_5 with $H_2O(s)$, magnifying the effects of the enhanced O_3 concentrations during the nighttime. Therefore, compared with November, in January the $PM_{2.5}$ concentrations experience a larger increase in NCP, and a smaller decline in the middle reach of the Yangtze River. As an integrated effect, the average $PM_{2.5}$ concentration reduction in ECH is smaller in January compared with November.

The annual average $PM_{2.5}$ concentration reductions under the 2015_ACT scenario (compared with the 2015_BAU scenario) are 1.23 μg m^{-3} (7.2%), 2.99 μg m^{-3} (7.7%), 3.27 μg m^{-3} (5.8%), 3.15 μg m^{-3} (4.7%), and 2.11 μg m^{-3} (5.9%) in the whole country, ECH, NCP, YRD, and PRD, respectively (Table 2), 65%, 65%, 71%, 83%, and 47% higher than the corresponding reductions from the 2015_BAU scenario to the 2015_REF scenario. Given that the NO_x emission reduction in the 2015_ACT scenario (compared with 2015_BAU scenario) are 45% higher than that of the 2015_REF scenario, the reduction of $PM_{2.5}$ concentrations per unit NO_x emission reduction increases as more stringent NO_x control measures are implemented.

4.2. Impact of the joint controls of NO_x and SO_2 on particulate matter pollution

As documented in Section 2.2, the SO_2 emissions are expected to be reduced by 18.9% from the 2015_REF scenario to the 2015_REF_SC scenario. Fig. 5 illustrates the reductions of $PM_{2.5}$ concentrations from the 2015_REF scenario to the 2015_REF_SC scenario. Due to the SO_2 emission reductions, the annual mean $PM_{2.5}$ concentrations decline by 1.5–5 μg m^{-3}, i.e. 2.1%–6.3%, in the majority of NCP and the middle and lower reaches of the Yangtze River, while the reductions are within 1.5 μg m^{-3} in other regions. Average $PM_{2.5}$ concentration reductions in ECH are 0.71 μg m^{-3}, 1.33 μg m^{-3}, 1.62 μg m^{-3}, and 1.24 μg m^{-3} in January, May, August, and November, respectively. The corresponding declining rates are 1.3%, 5.6%, 7.0%, and 2.5%, respectively. The $PM_{2.5}$ concentration reductions are the largest in August and the smallest in January, since higher temperature and stronger oxidation capacity favor the formation of sulfate. A detailed description of the effects of SO_2 emission control measures is given in the Supporting Information.

Fig. 5 also illustrates the benefit on $PM_{2.5}$ concentrations due to the joint controls of NO_x and SO_2 emissions requested by the governmental plan, namely the reductions of $PM_{2.5}$ concentrations from the 2015_BAU scenario to the 2015_REF_SC scenario. The annual mean $PM_{2.5}$ concentration decreases over 3 μg m^{-3}, i.e. 3.2%–13%, in the majority of ECH as a result of the joint controls. The middle and lower reaches of the Yangtze River experience $PM_{2.5}$ concentration reductions over 4.5 μg m^{-3}, i.e. 4.7%–13%, and some areas in the middle reach of the Yangtze River (mainly eastern Hubei, northern Hunan, and western Anhui) show reductions as large as 6–8.3 μg m^{-3}, i.e. 5.0%–13%. This spatial distribution of the $PM_{2.5}$ concentration reductions under the joint control measures shows a similar pattern with that under the NO_x control measures, as the reductions of $PM_{2.5}$ concentrations due to SO_2 control measures is relatively smaller and more uniformly distributed. The annual average $PM_{2.5}$ concentration reductions are 3.03 μg m^{-3}, 3.52 μg m^{-3}, 3.99 μg m^{-3}, and 2.80 μg m^{-3} in ECH, NCP, YRD, and

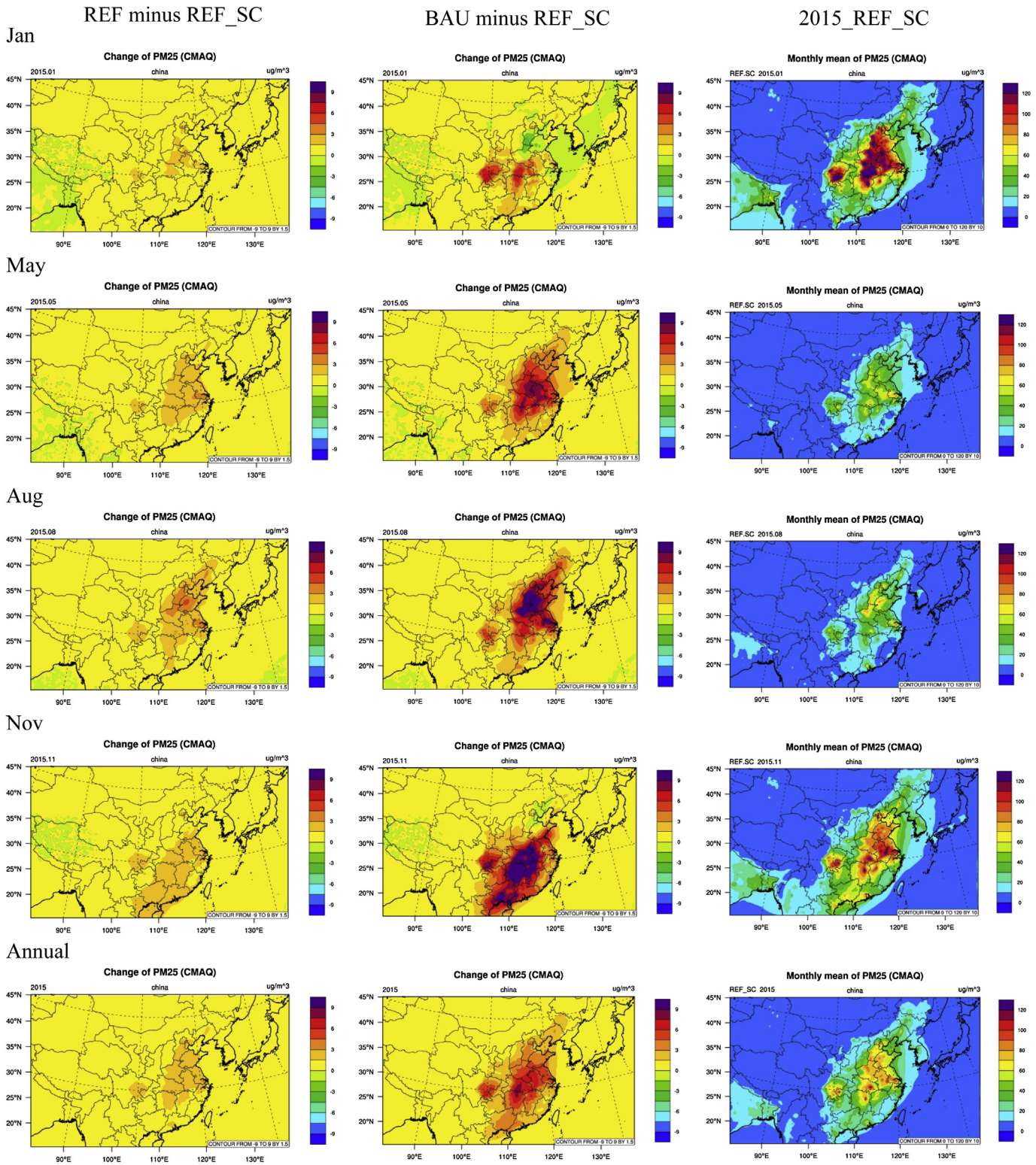

Fig. 5. The reductions of monthly (Jan, May, Aug, Nov) and annual mean $PM_{2.5}$ concentrations from the 2015_REF scenario to the 2015_REF_SC scenario (REF minus REF_SC, left column), from the 2015_BAU scenario to the 2015_REF_SC scenario (BAU minus REF_SC, middle column), and $PM_{2.5}$ concentrations under the 2015_REF_SC scenario (right column).

Table 3
The monthly (Jan, May, Aug, Nov) and annual mean concentrations of $PM_{2.5}$, sulfate, nitrate, ammonium, and ozone in 2010 and under four scenarios in 2015 (BAU, REF, ACT, REF_SC) over ECH, and the reductions between different scenarios.

Species[a]	2010	2015_BAU	2015_REF	2015_ACT	2015_REF_SC	BAU minus REF	BAU minus ACT	BAU minus REF_SC	REF minus REF_SC
Jan									
$PM_{2.5}$	52.93	53.34	52.84	51.88	52.14	0.50	1.46	1.20	0.71
SO_4^{2-}	5.37	5.56	6.05	6.26	5.34	−0.48	−0.70	0.22	0.70
NO_3^-	17.13	17.28	16.30	15.29	16.50	0.98	2.00	0.78	−0.20
NH_4^+	7.00	7.11	7.02	6.80	6.82	0.10	0.31	0.30	0.20
O_3	39.36	37.44	40.78	42.11	40.72	−3.34	−4.67	−3.29	0.06
May									
$PM_{2.5}$	24.33	25.79	23.98	23.07	22.65	1.81	2.72	3.14	1.33
SO_4^{2-}	5.44	5.74	5.94	5.98	4.99	−0.20	−0.25	0.75	0.95
NO_3^-	6.18	7.02	5.36	4.59	5.34	1.65	2.42	1.68	0.02
NH_4^+	3.84	4.19	3.79	3.58	3.43	0.41	0.61	0.77	0.36
O_3	54.01	54.43	53.50	52.58	53.49	0.93	1.85	0.95	0.01
Aug									
$PM_{2.5}$	23.13	24.94	22.98	22.07	21.36	1.96	2.87	3.57	1.62
SO_4^{2-}	6.15	6.66	6.74	6.75	5.59	−0.08	−0.09	1.07	1.15
NO_3^-	5.44	6.31	4.68	3.95	4.64	1.64	2.37	1.68	0.04
NH_4^+	3.89	4.34	3.89	3.68	3.45	0.45	0.66	0.89	0.44
O_3	50.42	51.74	49.11	47.44	49.18	2.63	4.30	2.56	−0.07
Nov									
$PM_{2.5}$	50.41	52.17	49.20	47.26	47.96	2.97	4.92	4.22	1.24
SO_4^{2-}	6.51	6.63	7.25	7.50	6.32	−0.62	−0.87	0.31	0.93
NO_3^-	17.38	18.66	15.61	13.81	15.64	3.05	4.85	3.02	−0.03
NH_4^+	7.51	7.93	7.27	6.84	6.94	0.65	1.08	0.99	0.34
O_3	45.03	43.76	46.30	47.10	46.25	−2.55	−3.34	−2.49	0.06
Annual									
$PM_{2.5}$	37.70	39.06	37.25	36.07	36.03	1.81	2.99	3.03	1.23
SO_4^{2-}	5.87	6.15	6.49	6.62	5.56	−0.35	−0.48	0.59	0.93
NO_3^-	11.53	12.32	10.49	9.41	10.53	1.83	2.91	1.79	−0.04
NH_4^+	5.56	5.89	5.49	5.23	5.16	0.40	0.67	0.74	0.33
O_3	47.21	46.84	47.42	47.31	47.41	−0.58	−0.47	−0.57	0.02

[a] The units of $PM_{2.5}$, SO_4^{2-}, NO_3^-, NH_4^+ are μg m^{-3}; the units of O_3 are ppb. The concentrations of O_3 are monthly/annual average daytime (12:00–18:00, local time) concentrations.

PRD, respectively (see Table 2), with declining rates of 7.8%, 6.2%, 5.9%, and 7.9%, respectively. The nation-wide control strategy does not induce obviously larger $PM_{2.5}$ concentration reductions in major city clusters, which are characterized by high population density, intensive economic activities, and severe air pollution. More stringent regional control policies are required for the significant improvement of particulate air quality in these city clusters. The annual average concentrations of sulfate, nitrate, and ammonium are reduced by 0.59 μg m^{-3}, 1.79 μg m^{-3}, and 0.74 μg m^{-3} under the joint control strategy. The reductions of nitrate concentrations are remarkably larger than sulfate, attributed largely to the trade-off increase of sulfate induced by the NO_x emission controls (see Section 4.1). Average $PM_{2.5}$ concentration reductions in ECH are 1.20 μg m^{-3}, 3.14 μg m^{-3}, 3.57 μg m^{-3}, 4.22 μg m^{-3} in January, May, August, and November, respectively. The corresponding declining rates are 2.3%, 12.2%, 14.3%, and 8.1%, respectively. The smallest reductions in January are consistent with the fact that January's reductions are the smallest under both NO_x and SO_2 control measures. In comparison, Fig. 4 illustrates that $PM_{2.5}$ pollution is the most severe in January in ECH, followed by

Table 4
The January mean values of gaseous pollutants and particulate matter concentrations and some chemical indicators under the 2015_BAU scenario and the 2015_REF scenario over NCP and YRD, and the concentration reductions from the 2015_BAU scenario to the 2015_REF scenario (BAU minus REF).

Species[a]	Unit	NCP			YRD		
		2015_BAU	2015_REF	BAU minus REF	2015_BAU	2015_REF	BAU minus REF
$PM_{2.5}$	μg m^{-3}	77.01	78.31	−1.30	85.52	86.25	−0.73
SO_4^{2-}	μg m^{-3}	5.34	5.89	−0.55	7.44	8.49	−1.04
NO_3^-	μg m^{-3}	23.26	23.59	−0.33	29.49	28.77	0.72
NH_4^+	μg m^{-3}	8.77	9.08	−0.31	11.50	11.69	−0.19
TN (=NO_3^- + HNO_3)	μg m^{-3}	23.62	23.81	−0.19	31.36	30.01	1.35
NO	ppb	5.89	3.74	2.15	5.82	2.89	2.94
NO_2	ppb	17.94	14.66	3.28	21.92	17.29	4.62
NH_3	ppb	10.88	10.66	0.22	7.38	7.40	−0.02
O_3	ppb	28.82	33.08	−4.26	30.69	39.36	−8.67
HO_x	ppb	0.22	0.51	−0.30	0.73	1.65	−0.92
N_2O_5	ppb	0.131	0.135	−0.004	0.048	0.059	−0.011
$H_2O_2/(HNO_3 + NO_3^-)$	–	0.04	0.04		0.02	0.02	
$O_3/(NO_Y - NO_x)$	–	16.61	17.41		9.33	11.13	
DSN	–	≈2	≈2		≈2	≈2	
GR	–	2.22	2.20		1.59	1.64	

[a] The concentrations of O_3 and HO_x are monthly/annual average daytime (12:00–18:00, local time) concentrations; while the concentrations of N_2O_5 are monthly/annual average nighttime (18:00–6:00, local time) concentrations.

November, May and August. More stringent policies should be implemented in winter to relieve the heavy pollution periods.

5. Conclusions

In 2010, the anthropogenic emissions of SO_2, NO_x, PM_{10}, $PM_{2.5}$, BC, OC, NMVOC and NH_3 in China were estimated to be 24.4 Mt, 26.1 Mt, 15.8 Mt, 11.8 Mt, 1.93 Mt, 3.51 Mt, 22.9 Mt, and 18.3 Mt, respectively. Based on current legislations and current implementation status (until the end of 2010), the NO_x and SO_2 emissions are projected to increase by 14.5% and 11.4% in 2015 from the 2010 levels, respectively. If the NO_x control measures requested by the governmental plan or more aggressive NO_x control measures are implemented during 2011–2015, the NO_x emissions are expected to decline by 12.2% and 23.9% from the 2010 levels (23.4% and 33.6% from the baseline projection). With the implementation of the SO_2 control measures requested by the governmental plan, the SO_2 emissions are expected to be 9.6% lower than those at the 2010 levels, and 18.9% lower than those of the baseline projection.

In the scenario of the planned NO_x control measures, the annual mean $PM_{2.5}$ concentrations decline by 1.5–6 μg m^{-3}, i.e. 1.6%–8.5%, in the majority of eastern China. The largest reduction occurs in the middle reach of the Yangtze River. Under accelerated NO_x control measures, the annual average $PM_{2.5}$ concentration reductions (compared with the baseline projection) in eastern China are 65% higher than the reductions under planned control measures. The unusual increase of $PM_{2.5}$ concentrations over NCP and YRD during January after the reductions of NO_x emissions was an integrated effect of excessive NO_x, the NH_3-rich inorganic aerosol chemistry, and the NMVOC-sensitive photochemical regime. Under the joint controls of NO_x and SO_2, the annual mean $PM_{2.5}$ concentrations decline over 3 μg m^{-3}, i.e. 3.2%–13%, in the majority of eastern China, and some areas in the middle reach of the Yangtze River have reductions as large as 6–8.3 μg m^{-3}, i.e. 5.0%–13%. The average $PM_{2.5}$ concentration reductions in eastern China are 1.20 μg m^{-3}, 3.14 μg m^{-3}, 3.57 μg m^{-3}, 4.22 μg m^{-3} in January, May, August, and November, respectively, with declining rates of 2.3%, 12.2%, 14.3%, and 8.1%, respectively.

The results of this study give very important implications for the development of air pollution control strategies. Both the controls of NO_x and SO_2 could relieve the particulate matter pollution in China to some extent. The joint control of NO_x and SO_2 could significantly enhance the air quality benefit. However, these control policies still have some limitations. The seasonal variation of $PM_{2.5}$ concentration reductions does not agree with the seasonal variation of the $PM_{2.5}$ concentrations in the base year, therefore more stringent policies should be implemented in winter. What's more, the nationwide control strategy does not induce obviously larger $PM_{2.5}$ concentration reductions in major city clusters. The $PM_{2.5}$ concentrations even increase in NCP and YRD during January, and in NCP during November. More stringent regional control policies are required for the significant improvement of particulate air quality in key regions. The reductions of $PM_{2.5}$ concentrations are partly compensated by the increase of sulfate induced from the NO_x controls. In order to mitigate this adverse effect of NO_x controls, we should either reduce NO_x emissions to a large extent, thereby altering the ozone chemistry from NMVOC-sensitive regime to NO_x-sensitive regime, or implement coordinated NMVOC emission reductions simultaneously.

Acknowledgments

This study is financially supported by the National Natural Science Foundation (21221004), special fund of State Key Joint Laboratory of Environment Simulation and Pollution Control (12L05ESPC), the MEP's Special Funds for Research on Public Welfares (No. 201009001), and the Program for New Century Excellent Talents in University (NCET-10-0532). We acknowledge the assistance of Ms. Melissa Allen in reviewing this paper.

Appendix A. Supplementary data

Supplementary data related to this article can be found at http://dx.doi.org/10.1016/j.atmosenv.2013.05.012.

References

China Association of Automobile Manufacturers, 2011. China Automotive Industry Yearbook 2011. China Commercial Publishing House, Beijing.
China Electricity Council, 2011. Annual Development Report of China's Power Industry. China Electric Power Press, Beijing (in Chinese).
Energy Research Institute in China (ERI), 2009. China's Low Carbon Development Pathways by 2050: Scenario Analysis of Energy Demand and Carbon Emissions. Science Press, Beijing (in Chinese).
Energy Research Institute in China (ERI), 2010. Guidebook for the Financing of Energy Efficiency and Renewable Energy Projects. China Environmental Science Press, Beijing (in Chinese).
Lei, Y., Zhang, Q.A., Nielsen, C., He, K.B., 2011. An inventory of primary air pollutants and CO(2) emissions from cement production in China, 1990–2020. Atmospheric Environment 45, 147–154.
Li, L., Chen, C.H., Fu, J.S., Huang, C., Streets, D.G., Huang, H.Y., Zhang, G.F., Wang, Y.J., Jang, C.J., Wang, H.L., Chen, Y.R., Fu, J.M., 2011. Air quality and emissions in the Yangtze River Delta, China. Atmospheric Chemistry and Physics 11, 1621–1639.
Lin, J., Nielsen, C.P., Zhao, Y., Lei, Y., Liu, Y., McElroy, M.B., 2010. Recent changes in particulate air pollution over China observed from space and the ground: effectiveness of emission control. Environmental Science & Technology 44, 7771–7776.
Lu, C.H., Chang, J.S., 1998. On the indicator-based approach to assess ozone sensitivities and emissions features. Journal of Geophysical Research – Atmospheres 103, 3453–3462.
Ministry of Environmental Protection of China (MEP), 2011. Bulletin of Urban Sewage Treatment Facilities, and Flue Gas Desulfurization/Denitrification Facilities of Coal-fired Power Plants, Beijing (in Chinese).
National Bureau of Statistics (NBS), 2011a. China Energy Statistical Yearbook 2011. China Statistics Press, Beijing.
National Bureau of Statistics (NBS), 2011b. China Industrial Economy Statistical Yearbook 2011. China Statistics Press, Beijing.
National Bureau of Statistics (NBS), 2011c. China Statistical Yearbook 2011. China Statistics Press, Beijing.
Seinfeld, J.H., Pandis, S.N., 2006. Atmospheric Chemistry and Physics, from Air Pollution to Climate Change. John Wiley & Sons, Inc., Hoboken, New Jersey.
Sillman, S., 1995. The use of NO_y, H_2O_2, and HNO_3 as indicators for ozone-NO_x-hydrocarbon sensitivity in urban locations. Journal of Geophysical Research – Atmospheres 100, 14175–14188.
Solomon, S., Qin, D., Manning, M., Chen, Z., Marquis, M., Averyt, K.B., Tignor, M., Miller, H.L., 2007. Climate Change 2007: the Physical Science Basis. Contribution of Working Group I to the Fourth Assessment Report of the Intergovernmental Panel on Climate Change. Cambridge University Press, Cambridge, United Kingdom and New York, NY, USA.
Streets, D.G., Fu, J.S., Jang, C.J., Hao, J.M., He, K.B., Tang, X.Y., Zhang, Y.H., Wang, Z.F., Li, Z.P., Zhang, Q., 2007. Air quality during the 2008 Beijing Olympic Games. Atmospheric Environment 41, 480–492.
Tsinghua University Building Energy Research Center (THUBERC), 2009. Annual Report on China Building Energy Efficiency. China Architecture & Building Press, Beijing (in Chinese).
van Donkelaar, A., Martin, R.V., Brauer, M., Kahn, R., Levy, R., Verduzco, C., Villeneuve, P.J., 2010. Global estimates of ambient fine particulate matter concentrations from satellite-based aerosol optical depth: development and application. Environmental Health Perspectives 118, 847–855.
Wang, L.T., Jang, C., Zhang, Y., Wang, K., Zhang, Q.A., Streets, D., Fu, J., Lei, Y., Schreifels, J., He, K.B., Hao, J.M., Lam, Y.F., Lin, J., Meskhidze, N., Voorhees, S., Evarts, D., Phillips, S., 2010a. Assessment of air quality benefits from national air pollution control policies in China. Part I: background, emission scenarios and evaluation of meteorological predictions. Atmospheric Environment 44, 3442–3448.
Wang, L.T., Jang, C., Zhang, Y., Wang, K., Zhang, Q.A., Streets, D., Fu, J., Lei, Y., Schreifels, J., He, K.B., Hao, J.M., Lam, Y.F., Lin, J., Meskhidze, N., Voorhees, S., Evarts, D., Phillips, S., 2010b. Assessment of air quality benefits from national air pollution control policies in China. Part II: evaluation of air quality predictions and air quality benefits assessment. Atmospheric Environment 44, 3449–3457.
Wang, L.T., Xu, J., Yang, J., Zhao, X.J., Wei, W., Cheng, D.D., Pan, X.M., Su, J., 2012. Understanding haze pollution over the southern Hebei area of China using the CMAQ model. Atmospheric Environment 56, 69–79.

Wang, Q.Y., 2011. Energy Data 2010 for the China Sustainable Energy Program. The Energy Foundation, Beijing (in Chinese).
Wang, S.X., Xing, J., Chatani, S., Hao, J.M., Klimont, Z., Cofala, J., Amann, M., 2011a. Verification of anthropogenic emissions of China by satellite and ground observations. Atmospheric Environment 45, 6347–6358.
Wang, S.X., Xing, J., Jang, C.R., Zhu, Y., Fu, J.S., Hao, J.M., 2011b. Impact assessment of ammonia emissions on inorganic aerosols in east China using response surface modeling technique. Environmental Science & Technology 45, 9293–9300.
Wang, S.X., Zhao, M., Xing, J., Wu, Y., Zhou, Y., Lei, Y., He, K.B., Fu, L.X., Hao, J.M., 2010c. Quantifying the air pollutants emission reduction during the 2008 Olympic Games in Beijing. Environmental Science & Technology 44, 2490–2496.
Wang, X.P., Mauzerall, D.L., Hu, Y.T., Russell, A.G., Larson, E.D., Woo, J.H., Streets, D.G., Guenther, A., 2005. A high-resolution emission inventory for eastern China in 2000 and three scenarios for 2020. Atmospheric Environment 39, 5917–5933.
Wei, X.L., Li, Y.S., Lam, K.S., Wang, A.Y., Wang, T.J., 2007. Impact of biogenic VOC emissions on a tropical cyclone-related ozone episode in the Pearl River Delta region, China. Atmospheric Environment 41, 7851–7864.
Zhang, Q., Streets, D.G., Carmichael, G.R., He, K.B., Huo, H., Kannari, A., Klimont, Z., Park, I.S., Reddy, S., Fu, J.S., Chen, D., Duan, L., Lei, Y., Wang, L.T., Yao, Z.L., 2009. Asian emissions in 2006 for the NASA INTEX-B mission. Atmospheric Chemistry and Physics 9, 5131–5153.
Zhang, X.Y., Wang, Y.Q., Niu, T., Zhang, X.C., Gong, S.L., Zhang, Y.M., Sun, J.Y., 2012. Atmospheric aerosol compositions in China: spatial/temporal variability, chemical signature, regional haze distribution and comparisons with global aerosols. Atmospheric Chemistry and Physics 12, 779–799.
Zhao, B., Wang, S.X., Xu, J.Y., Fu, K., Hao, J.M., Cofala, J., Klimont, Z., Amann, M., 2013. NO_x emission trends in China for the period 1995–2030. Atmospheric Chemistry and Physics (submitted for publication).
Zhao, Y., Wang, S.X., Duan, L., Lei, Y., Cao, P.F., Hao, J.M., 2008. Primary air pollutant emissions of coal-fired power plants in China: current status and future prediction. Atmospheric Environment 42, 8442–8452.